Geomechanics and Engineering, *Vol. 33, No. 6 (2023) 625-633*
https://doi.org/10.12989/gae.2023.33.6.625

Predicting soil-water characteristic curves of expansive soils relying on correlations

Ahmed M. Al-Mahbashi*, Muawia Dafalla[a] and Mosleh Al-Shamrani[b]

Bugshan Research Chair in Expansive Soils, Dept. of Civil Engineering, College of Engineering, King Saud Univ., Riyadh 11421, Saudi Arabia

(*Received May 5, 2022, Revised April 6, 2023, Accepted May 11, 2023*)

Abstract. The volume changes associated with moisture or suction variation in expansive soils are of geotechnical and geoenvironmental design concern. These changes can impact the performance of infrastructure projects and lightweight structures. Assessment of unsaturated function for these materials leads to better interpretation and understanding, as well as providing accurate and economic design. In this study, expansive soils from different regions of Saudi Arabia were studied for their basic properties including gradation, plasticity and shrinkage, swelling, and consolidation characteristics. The unsaturated soil functions of saturated water content, air-entry values, and residual states were determined by conducting the tests for the entire soil water characteristic curves (SWCC) using different techniques. An attempt has been made to provide a prediction model for unsaturated properties based on the basic properties of these soils. Once the profile of SWCC has been predicted the time and cost for many tests can be saved. These predictions can be utilized in practice for the application of unsaturated soil mechanics on geotechnical and geoenvironmental projects.

Keywords: expansive soils; index properties; prediction model; soil-water characteristic curve; unsaturated soil properties

1. Introduction

The most widespread problematic soils in arid and semi-arid areas are the expansive soils. The swelling nature causes damage of variable nature to light structures and pavements. Damage due to this type of soil is a major concern to property owners, governmental authorities, and researchers. Irreparable displacements in footings, minor to major cracks in walls and floors are common in light structures founded on highly plastic and expansive soils.

Slater (1983) provided an approximate guide to the suspected distribution and extent of potentially swelling soils in Saudi Arabia and places with the most severe problems in the Arabian Peninsula. The Bugshan research chair in expansive soils was established at King Saud University in the year 2007. Research provided by this chair covered many aspects of expansive soils. In Saudi Arabia, expansive soils are recognized in nine provinces out of 13 provinces. Major areas of occurrence of expansive soils are the areas where damage is significant. The places that suffer the most are Tabuk, Al-Ghatt, Al-Hafuf, and Al-Qatif. Other isolated locations beyond these zones include Sharoura, Obhour, and east Riyadh (Dafalla *et al.* 2017). The nature and origin of these soils vary from place to place in Saudi Arabia, but four groups can be identified (Dafalla and Al-Shamrani 2014). Shale material consisting of silty or clayey shale is the main group in the central and northern parts of the country (Al-Ghatt and Tabuk). The second group is the calcareous clay which is dominant in the eastern province (Hasa, Alhafouf, and Al-Qatif). The third group is the greenish clay widely encountered in Al Madina Almunawarah and close vicinity of (Tayma). This green clay usually overlies decomposed igneous rock. Reddish silty clay is the fourth group, which consists of a combination of windblown and alluvial deposits (Najran and Sharorah).

Occurrence of these formations in semiarid nature or as manmade compacted layers typically existed in an unsaturated state. Mostly compacted layers are reconstituted to be used as liners, buffer materials in radioactive waste, embankment, and other geotechnical-geoenvironmental projects. Advanced and high-technical studies are currently presented in the field of unsaturated soil which assist in the investigation and the prediction of expansive soil behavior.

Laboratory-based and computations-based prediction models are now popular in unsaturated soil mechanics and frequently used in geotechnical and geo-environmental practice. There is a growing interest in using soil-water characteristic curve (SWCC) design models to describe the behavior of unsaturated soils. It is also used as a valuable tool for the design and analysis of slopes, pavements, retaining walls, shallow foundations as well as other components of infrastructure projects (Tavakkoli and Vanapelli 2011, Liu and Vanapalli 2019, Rahardjo *et al.* 2019, Rong *et al.* 2021, Chen *et al.* 2021, Mounika *et al.* 2023).

*Corresponding author, M.Sc
E-mail: aalmahbashi@ksu.edu.sa;
ena_almahpashi@hotmail.com
[a]Associate Professor
[b]Professor

ISSN: 2005-307X (Print), 2092-6219 (Online)

Soil water characteristic curve SWCC defines the relationship between water content (gravimetric, volumetric, or degree of saturation) and soil suction, (u_a–u_w). The shape of SWCC could be unimodal or bimodal (as shown in Fig. 1) and this depends on the series of pores (micro and macropores) that soil possesses (i.e., Durner 1994, Tuller *et al.* 1999, Burger and Shackelford 2001, Zhang and Chen 2005). The unimodal SWCC is sigmoid and has three identifiable key variables: saturated volumetric water content, θ_s, air-entry value, AEV, and residual volumetric water content, θ_r. The air-entry value is defined as the value of suction when the air starts to enter the large soil pores. The residual water content (θ_r) is defined as the amount of water that is tightly attached to soil particles and an increase in suction corresponds to an insignificant change in water content. These points divide the profile of SWCC into three zones; saturated or boundary effect zone, transition zone, and residual zone (Vanapalli *et al.* 1996, Fredlund *et al.* 2012). In the first zone, the soil pores are almost filled with water and are governed by the capillary action, and when suction reaches beyond AEV the transition zone starts with the desaturation of water from the largest pores. At the residual state, the liquid phase inside the pores becomes discontinuous and tightly attracted to soil particles. In the bimodal shape of SWCC, the curve is characterized by two distinct air-entry values (AEV1 and AEV2) and two distinct residual water contents (θ_{r1}, θ_{r2}). Based on these points, the transition stage could be divided into macro-transition and micro-transition zone (Satyanaga *et al.* 2013). The shape of SWCC has been affected by fine percent, additives such lime or cement addition which alter the pores series, while inert materials such as fibers introduce a marginal effect (Elkady *et al*. 2015, Elkady *et al.* 2017, Al-Mahbashi *et al.* 2020).

Numerous fitting models have been developed to construct a continuous profile of SWCC based on the parameters related to laboratory-measured points and identify the main properties of unsaturated soils such as air-entry value (AEV) and residual state (Fredlund and Xing 1994, Pham and Fredlund 2008).

Other empirical models were developed to predict soil-water characteristic curves based on the physical properties of particle size distribution curves and SWCC variables (i.e., Satyanaga *et al.* 2013, Zhai *et al.* 2020). Recently, Li and Vanapalli (2021) introduced an equation to predict the bimodal soil-water characteristic curve, this equation was developed based on the characteristics of the pore size distribution curve and volumetric water content in macropores and micropores in a different stage. Chin *et al.* (2010) proposed a method to predict the bimodal SWCC using the empirical correlations, based on the fitting parameters Fredland and Xing equations and D50 for particle size. This method was found to be applicable for coarse and fine-grained soils, this method required laboratory point measurements of suction (i.e., between 10 to 500 kPa).

Atterberg limits are related to the mineralogical composition of the soil, pore fluid chemistry, and type of adsorbed cation (Mitchell and Soga 2005), and all these variables govern the suction characteristics of soil (Lu and Khorshidi 2015). Fredlund *et al.* (2011) suggested that there

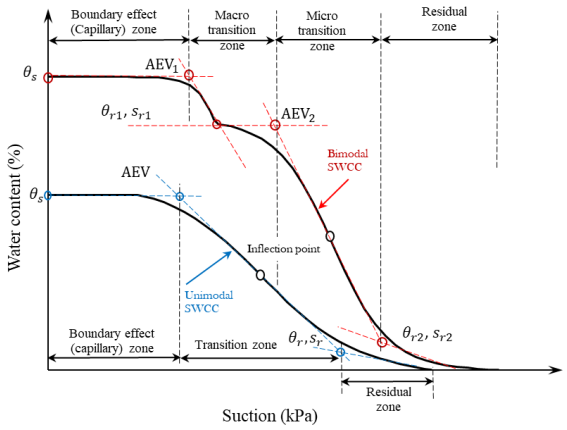

Fig. 1 Typical bimodal and unimodal SWCC

is a correlation between shrinkage limit and residual water content as well as air-entry value with the plastic limit for fine-grained soils. Al-Mahbashi *et al*. (2015) investigated correlation trends for the variation of shrinkage limit (w_{Sh}), plastic limit (w_P), residual water content, and air-entry value for expansive soil with different additions of lime. The study revealed that the shrinkage limit and residual water content show similar trends as for the plastic limit and air-entry value when correlated to each other. In a similarity, Lu and Dong (2017) have interpreted the different stages of the shrinkage curve (normal, residual and zero shrinkage) for fine-grained soils in light of capillary force and adsorption mechanism and showed how it is correlated to the soil-water characteristic curve.

The correlation between basic properties or index properties of soil with soil water characteristics is not well covered in the literature and requires more investigation to simplify the applications of unsaturated soil models. In this study, a simplified method has been proposed to predict the main characteristics of bimodal SWCC (i.e., controlling points) for fine-grained soils based on the regression analysis for data measured in the laboratory. Then, the SWCC profile could be constructed graphically or using fitting equations. A new prediction tool enables the practice geotechnical engineers to build an SWCC from the routine tests normally carried out in laboratories. When the profile of SWCC has been predicted the time and cost for many tests can be saved. These predictions can be utilized in the assessment of unsaturated soil mechanics and many geotechnical and geoenvironmental parameters.

2. Materials used

Expansive soils from different areas of Saudi Arabia were collected from excavated shallow test pits (1.0 - 2.5m) below the ground surface. The collected materials were pulverized after air drying and sieved through sieve # 40.

The samples selected for this study included most of the types of expansive soils present in Saudi Arabia. The type originated from shale and claystone including Ghatt, Zulfi, Hudaiba, Al Quliba, and Tabuk. The type that originated from the calcareous formation includes Hafuf, Hasa,

Table 1 Basic properties of soils utilized on this study

Soil/Property	Specsific Gravity, Gs	Liquid Limit, w_L (%)	Plastic limit, w_P (%)	Shrinkage limit, w_{Sh} (%)	Optimum moisture content, %	Maximum dry density, kN/m2
Hafuf (Hf)	2.7	37.0	27.0	23.0	16.0	17.3
Hasa (Hs)	2.7	23.0	16.0	21.0	13.0	18.4
Hazm (Hzm)	2.8	50	39	17.5	19.0	16.7
Hudaibah (Hb)	2.7	33.0	23.0	16.0	14.3	17.6
Taymaa (Tm)	2.7	32.0	22.9	25.0	16.5	17.3
Zulfi (Zf)	2.8	30.0	18.8	14.0	16.0	17.8
Hazm_BG (Hzm-BG)	2.8	79.0	39.0	15.0	34.0	13.4
AlQulibah (Qb)	2.8	32.0	20.0	17.0	14.3	18.3
Ghatt (Gt)	2.9	59.3	33.0	14.0	24.7	16.0
Al-Qatif (Qf)	2.7	160.0	60.0	15.0	38.0	11.8
Tabuk (Tk)	2.8	43.0	27.0	21.0	17.0	16.6
Qf2L	2.7	120.1	87.7	17.3	42.0	11.4
Qf4L	2.7	96.0	85.0	19.7	44.0	11.0
Qf6L	2.7	96.8	86.4	20.0	46.0	10.8

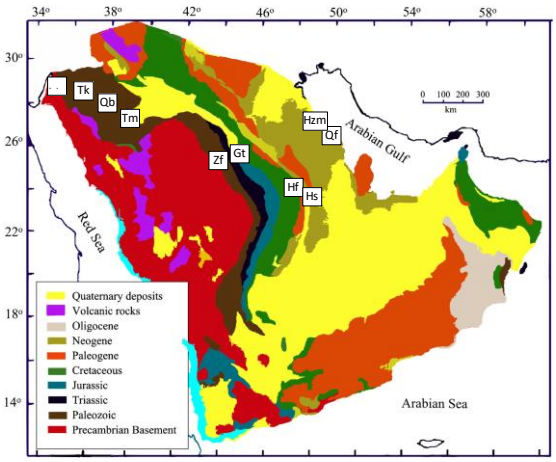

Fig. 2 Geological map with study areas

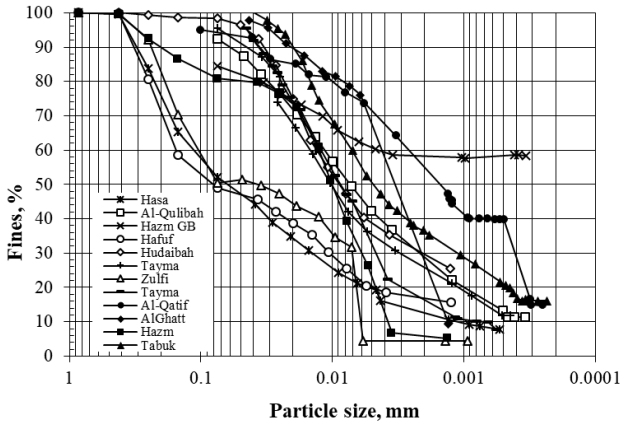

Fig. 3 Geological map with study areas

Hazam, Hazam (BG), and Al-Qatif. A green clay sample was taken from Tayma. The total number is 12 samples covering the most commonly known areas in Saudi Arabia. The geological map of the Arabian Peninsula is presented in Fig. 2, the rock formations and locations are presented also in this map.

3. Experimental program

3.1.Basic characterization

The tests conducted here were required to perform the geotechnical characterization according to the American Society of Testing and Materials (ASTM). Geotechnical characterization included specific gravity (ASTM-D854, ASTM 2014a), Atterberg limits (ASTM-D 4318, ASTM 2017), and standard proctor compaction (ASTM-D698, ASTM 2012).

Al-Qatif clay is extremely high plasticity clay and in order to obtain a plasticity index (PI) that bridges the gap to other soils which are generally low to medium plasticity three other samples were considered. These are obtained by the addition of 2%, 4%, and 6% of lime and marked in this study as Qf2%L, Qf4%L, and Qf6%L respectively. The lime addition has been proven to induce notable stabilization due to the fabric alteration of this soil (Al-Mahbashi 2014, Al-Mahbashi *et al*. 2015).

The grain size distribution tests including both sieve analysis (ASTM-D6913, ASTM 2009) and hydrometer analysis ASTM-D7928 (ASTM 2021) were performed in the laboratory for all samples. The particle size distribution curves for tested soils were presented in Fig. 3. The soil with bimodal grain size distribution may exhibit unimodal or bimodal SWCC, and this depends on other factors such as soil structure and density (Satyanaga *et al.* 2013).

3.2 Swelling and Consolidation characteristics

The swelling and consolidation characteristics were determined for the different soils using the one-dimensional oedometer device following ASTM-D4546 (ASTM 2014b) and ASTM-D2435 (ASTM 2011). Statically compacted specimens at optimum molding conditions of optimum water content and maximum dry density (Table 1) were prepared for this purpose, the specimens were in 64 mm diameter and 16 mm in height. The specimens were initially inundated on the oedometer cell and allowed to swell under light surcharge load (i.e., 7kPa), when the swell diminished the specimens start to load incrementally to return to their initial height and consolidated up to 800 kPa. Then the load was reduced back to draw the rebound curve.

3.3 Soil water characteristic curves

Two different techniques were used in this study to obtain the drying SWCC along with the entire range of suction. These techniques included axis translation techniques (ATT) for the suction range less than 1.5 MPa (ASTM-D6836, ASTM 2016a), and contact filter paper technique (CFPT) for measuring the soil suction more than 1.5 MPa (ASTM-D5298, ASTM 2016b). The first technique utilized Fredlund SWCC-devise to apply matric suction on the saturated specimen was gently placed on the top of the saturated high air-entry value (HAEV) ceramic disk. This disk allows only for water to flow by separating the air and water phases. Under the HAEV disk, there is a compartment filled with water to ensure contact of water with the soil specimen. Several studies have been conducted using this device (i.e., Al-Mahbashi and Elkady 2017, Al-Mahbashi *et al.* 2021), and more details about the device component are available in Pham *et al*. (2004) and Al-Mahbashi (2014). The compacted specimens were saturated under a low surcharge load (i.e., 7 kPa), and this process was conducted on an oedometer cell where the cell is connected to a dial gauge to trace vertical strain during saturation. Saturated specimens were placed above the saturated HAEV disk with good contact to ensure the continuity of water. Matric suction was imposed by applying air pressure in successive sequents up to 1500 kPa (i.e., 5, 10, 20, 50, 100, 200, 400, 800, and 1500 kPa). The specimen is connected to a linear variable differential transducer (LVDT) connected to a data logger, to trace vertical deformations during the suction application, radial deformation was measured using the image processing technique (Elkady and Almahbashi 2012) or digital caliper (0.01 mm) and volume changes taking place were computed. The water expelled from the soil specimen was collected in the compartment below HAVE disk, two graduated burettes were also connected to this compartment to monitor the volume of expelled water. The equilibrium under each suction increment was assumed when there is no more water expelled during the day and there is no change in the vertical strain.

The Contact Filter Paper Technique (CFPT) was used for suction in excess of 1,500 kPa as the axis translation procedure would not be suitable due to the ceramic disk suction level tolerance. CFPT was considered to cover the zone with a suction of more than 1,500 kPa. This is needed to evaluate the general trend of the SWCC over a high suction range (up to 100 MPa). The measurement of matric suction was not direct and required samples of predetermined water content. A series of compacted disk specimens need to be conditioned at variable water content. This was attained by drying or wetting of compacted specimens to achieve the required water content. The drying or wetting was conducted in a controlled approach to simulate natural gain or introduction of water to the subsoil material. To reach to specific moisture content, sufficient time is allowed and this may reach five days.

The sample is placed in a humid container to achieve the required wetting. Then the sample is stored in a humidity-controlled chamber. Wetting is achieved by placing the samples in a humid environment. Oven-dried filter paper, Whatman No. 42, was placed between two identical disc specimens. A calibrated chart for the filter paper showing suction corresponding to each moisture level is established. Details about this method are given in more detail by Al-Mahbashi *et al*. (2017). The two-disc samples were 70 mm in diameter, while the filter paper placed in the middle was 50 mm in diameter. A seating load of 7 kPa was applied to ensure contact between the filter paper and the soil samples. At least 20 days were allowed for the entire setup placed inside a sealed glass jar. This is expected to ensure moisture equilibration between the filter paper and the disk specimen.

4. Results and discussion

4.1 Basic properties

The grain size distribution for 12 clay materials tested was presented in Fig. 3, the drawn curves indicated that fine material passing sieve size 0.002 mm in a range of 5% to 58%. The trend of particle size is almost similar to HZM GB clay indicating more fines and Zulfi clay with the lowest fine content. The optimum moisture content varied from 13% to 25% approximately for most of the tested clay except for Al-Qatif and Hazm GB where values of more than 30% are reported. Lime-treated Al-Qatif clay reported optimum moisture content of more than 40%. The corresponding maximum dry density was reported in a range of 11.80 kN/m^3 to 18.40 kN/m^3. The low dry density is associated with the highly plastic clay from the eastern parts of Saudi Arabia. Treatment with lime resulted in an extra lightweight clay material with a dry density close to 10 kN/m^3. The shrinkage limit varied from 14 to 23% for all tested clays. The liquid limit (w_L)varied from 23 to 160 indicating a wide range of plasticity. The specific gravity was obtained in a range of 2.7 to 2.9.

4.2 Swelling and consolidation

The materials used in this study belong to soils that possess low to high swelling potential, the swelling and consolidation characteristics for these soils are key properties and addressed in this section for characterization purposes.

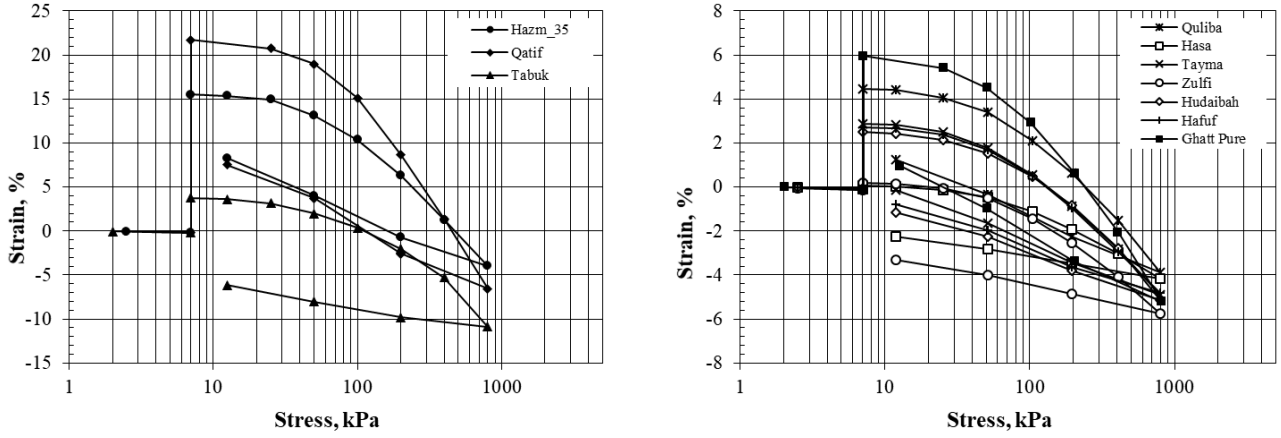

(a) (b)

Fig. 4 Swelling and consolidation characteristics of expansive soils

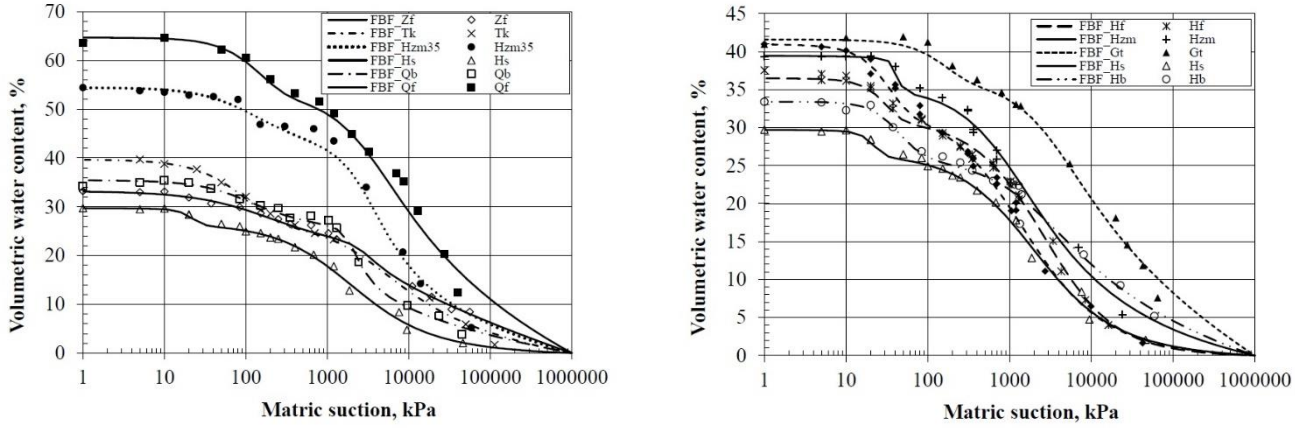

(a) (b)

Fig. 5 (a) and (b) Soil water characteristics curves for selected soils

The swelling and consolidation tests performed on the clay samples are presented in Figs. 4(a) and 4(b). It can be observed that Hazam and Qatif present a higher swell strain in the range of 15% to 20%, and steep slope compressibility. The Tabuk swell strain is less than 5% (Fig. 4(a)). The swell and compressibility curves indicated in Fig. 4(b) showed a swell strain variation from less than 1 to 6% for all other clays not shown in Fig. 4(a). The compression curves are generally converging toward stress of 800 kN/m^2. Most of the shown clays are overconsolidated except for Tayma and Qulaiba clay.

4.3 SWCC and unsaturated soil properties

The results of SWCC obtained after combining the axis translation technique and the filter paper technique are presented in terms of volumetric water content versus matric suction. The volumetric water content (θ) is defined as the volume of water inside soil pores referenced to the instantaneous total volume of the soil. The results show bimodal shapes for the selected materials in this study. Bimodal fitting equation proposed by Fredlund (1999) was used to fit the laboratory data through SoilVision software as shown in Figs. 5(a) and 5(b). The results show a variety of retention capacities (the ability of soil to hold water) for selected soils; saturated volumetric water contents werewithin the range of 28% to 68%, the AEV_1 and AEV_2 were in the range of 10 to 70 kPa and 100 to 1300 kPa respectively. The variation in retention capacity is attributed mainly to the mineralogical composition of soil; Qf soil shows the highest retention capacity and this soil possess a considerable amount of montmorillonite reaching about 33% (Rafi, 1988). The fines percent could alter the retention capacity and the shape of SWCC due to the change in the filled-up openings geometry and the overall pores sizes (Raghuram *et al*. 2020; Dafalla and Al-Mahbashi 2020, Al-Mahbashi *et al*. 2021). This variety will be utilized to provide a prediction model in correlation to the basic properties of these soils.

4.4 Prediction model of unsaturated soil properties

The main characters of SWCC or control points including AEVs and residual state variables have been determined using the graphical methods (Vanapalli *et al.* 1998, Satyanaga *et al.* 2013) and represent the points of

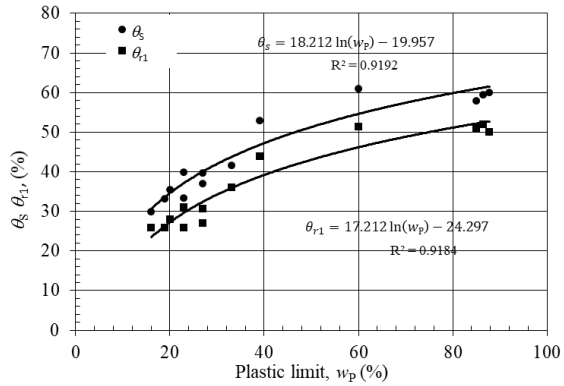

Fig. 6 Correlation between saturated and residual water content with w_P

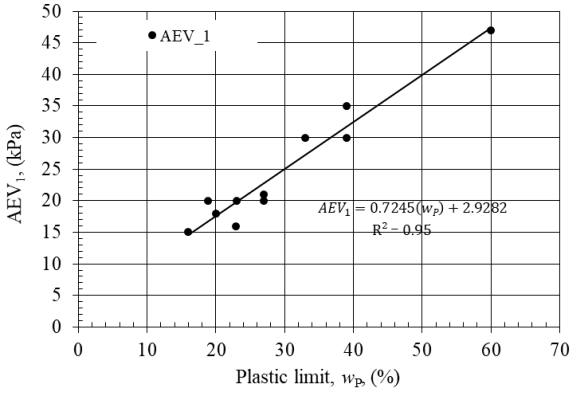

Fig. 7 Correlation between AEV_1 with w_P

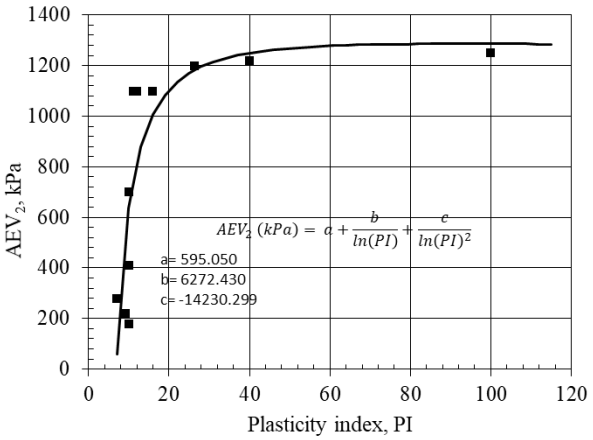

Fig. 8 Correlation between AEV_1 with PI

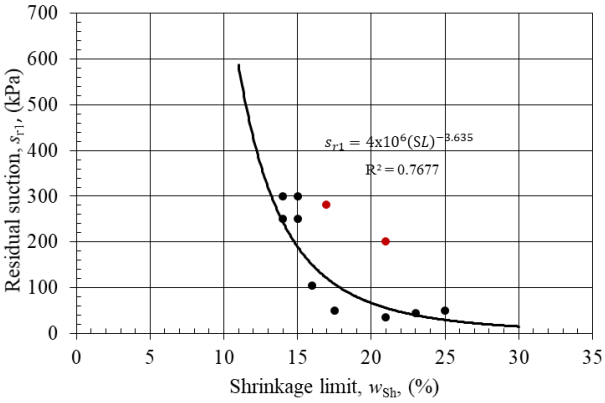

(a)

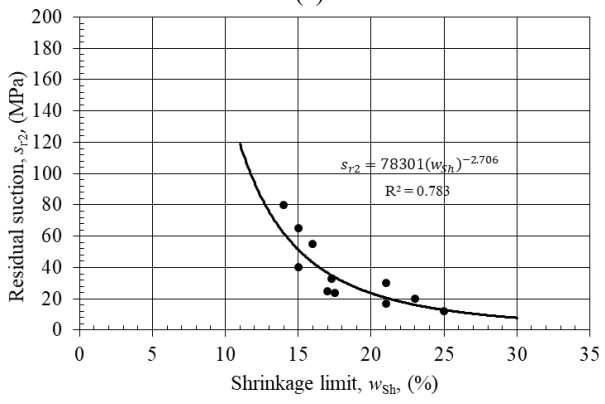

(b)

Fig. 9 Correlation between (a) residual suction, s_{r1} and (b) residual suction s_{r2} with w_{Sh}

intersection of tangents to the saturation zone, transition zones, and residual zone. As mentioned earlier, the SWCC depends on index properties such as shrinkage limit, plastic, and also liquid limit (Mitchell and Soga 2005, Fredlund *et al.* 2011, Al-Mahbashi *et al*. 2015). Wijaya *et al*. (2015) defined the shrinkage state to be used in the determination of air-entry value. The characteristics of the shrinkage curve were shown to have a significant role in the determination of air-entry value, especially the minimum void ratio of the shrinkage curve. Lu *et al*. (2017) also revealed that the shrinkage rate at the drying path is strongly correlated to the characteristics of SWCC. Villar *et al*. (2009) either showed the convergence of the plastic limit to an air-entry value in the process of soil drying. The variation of the plastic limit for different clays is less than the variation of the liquid limit. Zhou and Lu (2021) found that the Atterberg limits for fine-grained soils were well linked to the mechanisms of soil-water interaction.

The correlations between basic properties and unsaturated characteristics as obtained from SWCC were developed using regression analysis and the best-fit formulas were selected as shown in Figs. 6-10. These correlations have been written in equations 1 to 7, and show good to excellent power. Five main points related to AEVs, residual water contents and residual suctions were predicted using these equations as shown in Fig. 11. The point of saturated water content (θ_s) could be also easily measured in the lab for saturated specimens by the determination of gravimetric water content. The water content of the soil is set equal to zero when suction of soil reaches the maximum suction value of 10^6 kPa (Richards 1965), hence, the last point of the initiated profile was proposed as (0%, 10^6 kPa).

$$\theta_s = 18.212\ln(w_P) - 19.957 \quad (1)$$

$$AEV_1(kPa) = 0.7245(\mathrm{Pl}) + 2.9282 \quad (2)$$

$$\theta_{r1} = 17.212\ln(w_P) - 24.297 \quad (3)$$

$$s_{r1} = 4x10^6(w_{Sh})^{-3.635} \quad (4)$$

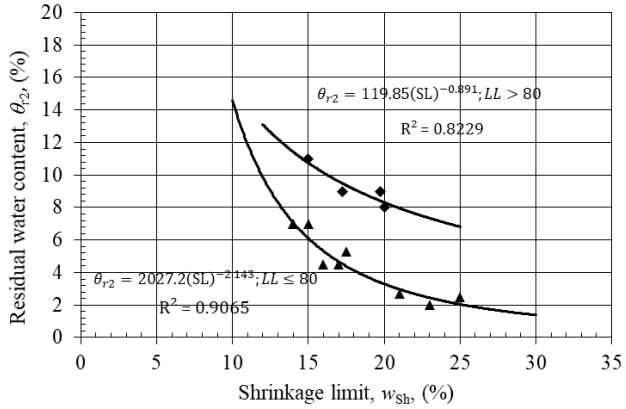

Fig. 10 Correlation between residual water content, θ_{r2} with w_{Sh}

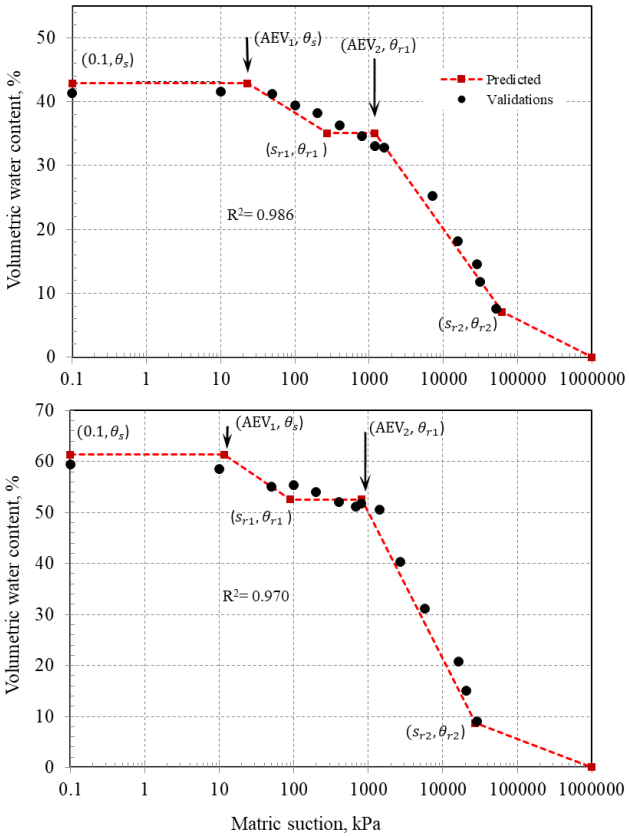

Fig. 11 Predicted profile of SWCC and validation points

$$\begin{cases} \theta_{r2} = 119.85(w_{Sh})^{-0.891}; & LL > 80 \\ \theta_{r2} = 2027.2(w_{Sh})^{-2.143}; & LL \leq 80 \end{cases} \quad (5)$$

$$AEV_2\ (kPa) = a + \frac{b}{ln(PI)} + \frac{c}{ln(PI)^2} \quad (6)$$

a= 595.050, b= 6272.430 and c= -14230.299

$$s_{r2}(MPa) = 78301(w_{Sh})^{-2.706} \quad (7)$$

From the above, it can be seen that the SWCC can be constructed based on the control points computed from Eqs. (1) to (7) as shown in Fig. 11 with two validation cases (cases 1 and 2). Fig. 11 presents a typical SWCC to be used for the clay under investigation with an excellent power R^2 of more than 0.9. When the basic index parameters vary within the same site more than one envelope of the SWCC can be plotted and average lines can be constructed to represent a single curve. This procedure can be adopted for all unsaturated soils within the arid and semi-arid zone of Saudi Arabia. Also from this study, SWCC is established for 12 clays known in Saudi Arabia. Adjustments can be considered when the clay within an area varies with respect to its index properties. Further studies are recommended to include more expansive soil formations and improve the correlations obtained.

5. Conclusions

This research study introduced the soil-water characteristic curves for (12) locations distributed all over the Kingdom of Saudi Arabia. It also presented a prediction method that can establish the control points of the SWCC graphs based on the index properties commonly tested as routine in practice. Seven prediction equations were derived for clays that are dominant in the region were used to establish reliable SWCC envelopes. The control points including the air entry value and residual state variables expressed in volumetric moisture content are introduced in terms of liquid limit, plastic limit, plasticity index, and shrinkage limit. These were found sufficient to build both unimodal and bimodal fittings commonly adopted for the SWCC profiles of unsaturated clays. When the profile of the SWCC has been predicted the time and cost for testing can be reduced. This study indicated that the residual suction and the saturated moisture content can be expressed in terms of the natural logarism of the plastic limit. The residual suction and residual moisture content can be both given as: $m(W_{sh})^n$. For example, for suction 2 in a bimodal fitting the m factor is estimated as 78301 and n is estimated as 2.706. The residual moisture content can be expressed in a similar way where m is estimated at 119.8 and n at –0.891. The Air entry value was found a linear function in the plasticity index for the first part of the SWCC and assumes a different trend for the second part of the SWCC. It is recommended that practicing engineers can utilize this prediction technique in the design of the geotechnical and geoenvironmental projects related to expansive soils of this semi-arid region.

Data availability

All data, models, and code generated or used during the study appear in the submitted article.

Declaration of competing interest

The authors declare that they have no known competing financial interests or personal relationships that could have appeared to influence the work reported in this paper.

Acknowledgments

The authors extend their appreciation to the Deanship of Scientific Research, King Saud University, for funding this research through the Vice Deanship of Scientific Research Chairs, Research Chair of Bugshan Research Chair in Expansive Soils.

References

Al-Mahbashi, A.M., Al-Shamrani, M.A. and Abbas, M.F. (2021), "Hydromechanical behavior of unsaturated expansive clay under repetitive loading", *J. Rock Mech. Geotech. Eng*., **13**(5), 1136-1146. https://doi.org/10.1016/j.jrmge.2021.05.002.

Al-Mahbashi, A.M., Al-Shamrani, M.A., Dafalla, M. and Basu, D. (2021), "Effect of temperature on hysteretic behavior of water retention capacity for clay–sand liners", *Indian Geotech. J*., **51**, 924-934. https://doi.org/10.1007/s40098-020-00469-5.

Al-Mahbashi, A.M., Al-Shamrani, M.A. and Moghal, A.A.B. (2020), "Soil–water characteristic curve and one-dimensional deformation characteristics of fiber-reinforced lime-blended expansive soil", *J. Mater. Civil Eng*., **32**(6), 04020125. https://doi.org/10.1061/(ASCE)MT.1943-5533.0003204.

Al-Mahbashi, A.M. and Elkady, T.Y. (2017), "Prediction of unsaturated shear strength of expansive clays", *Proceedings of the Institution of Civil Engineers-Geotechnical Engineering*, **170**(5), 407-420. https://doi.org/10.1680/jgeen.16.00037.

Al-Mahbashi, A.M., Elkady, T.Y. and Alrefeai, T.O. (2015), "Soil water characteristic curve and improvement in lime treated expansive soil", Geomech. Eng., **8**(5), 687-706. https://doi.org/10.12989/gae.2015.8.5.687.

Al-Mahbashi, A.M. (2014), "Soil Water Characteristic Curves of Treated and Untreated Highly Expansive Soil Subjected to Different Stresses", MS.c. Thesis; King Saud University, Riyadh, Saudi Arabia.

ASTM (2009), ASTM D6913-09: Standard Test Methods for Particle-Size Distribution (Gradation) of Soils Using Sieve Analysis. ASTM International, West Conshohocken, PA, USA.

ASTM (2011), ASTM D2435-11: Standard Test Methods for One-Dimensional Consolidation Properties of Soils Using Incremental Loading. ASTM International, West Conshohocken, PA, USA.

ASTM (2012), ASTM D698-12: Standard test methods for laboratory compaction characteristics of soil using standard effort (12 400 ft-lbf/ft3 (600 kN-m/m3)). ASTM International, West Conshohocken, PA, USA.

ASTM (2014a), ASTM D854-14: Standard test methods for specific gravity of soil solids by water pycnometer. ASTM International, West Conshohocken, PA, USA.

ASTM (2014b), ASTM D4546-14: Standard test methods for one-dimensional swell or collapse of cohesive soils. ASTM International, West Conshohocken, PA, USA.

ASTM (2016a), ASTM D6836-16: Standard test methods for determination of the soil water characteristic curve for desorption using a hanging column, pressure extractor, chilled mirror hygrometer, and/or centrifuge. ASTM International, West Conshohocken, PA, USA.

ASTM (2016b), ASTM D5298-16: Standard test method for measurement of soil potential (suction) using filter paper. ASTM International, West Conshohocken, PA, USA.

ASTM (2021), ASTM D7928-21: Standard Test Method for Particle-Size Distribution (Gradation) of Fine-Grained Soils Using the Sedimentation (Hydrometer) Analysis, ASTM International, West Conshohocken, PA, USA.

ASTM (2017), ASTM D4318-17: Standard test methods for liquid limit, plastic limit, and plasticity index of soils. ASTM International, West Conshohocken, PA, USA.

Burger, C.A. and Shackelford, C.D. (2001), "Soil-water characteristic curves and dual porosity of sand–diatomaceous earth mixtures", *J. Geotech. Geoenviron. Eng*., **127**(9), 790-800. https://doi.org/10.1061/(ASCE)1090-0241(2001)127:9(790).

Chen, X., Zhang, L., Zhang, L., Zhou, Y., Ye, G. and Guo, N. (2021), "Modelling rainfall-induced landslides from initiation of instability to post-failure", *Comput. Geotech*., **129**, 103877. https://doi.org/10.1016/j.compgeo.2020.103877.

Chin, K.B., Leong, E.C. and Rahardjo, H. (2010), "A simplified method to estimate the soil-water characteristic curve", *Can. Geotech. J*., **47**(12), 1382-1400. https://doi.org/10.1139/T10-033.

Dafalla, M.A. and Al-Mahbashi, A.M. (2020), Effect of adding natural clay on the water retention curve of sand-bentonite mixtures. In Unsaturated Soils: Research & Applications (pp. 1017-1022). CRC Press.

Dafalla, M.A. and Al-Shamrani, M.A. (2014), "Swelling characteristics of Saudi Tayma shale and consequential impact on light structures", *J. Civil Eng.Architect*., **8**(5), 613-623. http://www.davidpublisher.com/Public/uploads/Contribute/5549e55a3f95d.pdf.

Dafalla, M., Al-Shamrani, M. and Al-Mahbashi, A. (2017), "Expansive soil foundation practice in a semiarid region", *J. Perform. Constr. Fac*., **31**(5), 04017084. https://doi.org/10.1061/(ASCE)CF.1943-5509.0001078.

Durner W. (1994), "Hydraulic conductivity estimation for soils with heterogeneous pore structure", *Water Resour. Res*., **30**(2), 211-223. https://doi.org/10.1029/93WR02676.

Elkady, T.Y. and Al-Mahbashi, A.M. (2012), "Effect of vertical stress on the soil water characteristic curve of highly expansive", *Proceedings of the 2nd European Conf. on Unsaturated Soils: Research and Applications*, Berlin, Germany, June. https://doi.org/10.1007/978-3-642-31116-1_22.

Elkady, T.Y., Al-Mahbashi, A., Dafalla, M. and Al-Shamrani, M. (2017), "Effect of compaction state on the soil water characteristic curves of sand–natural expansive clay mixtures", *Eur. J. Environ. Civil Eng*., **21**(3), 289-302. https://doi.org/10.1080/19648189.2015.1112844.

Fredlund, D.G. and Xing, A. (1994), "Equations for the soil-water characteristic curve", *Can. Geotech. J*., **31**(4), 521-532. https://doi.org/10.1139/t94-061.

Fredlund, D.G., Rahardjo, H. and Fredlund, M.D. (2012), "Unsaturated Soil Mechanics in Engineering Practice", John Wiley and Sons, Inc., New York, USA.

Fredlund, D. G., Stone, J., Stianson, J. and Sedgwick, A. (2011), "Obtaining unsaturated soil properties for high volume change oil sands material", *Proceedings of the 5th Asia Pacific Conference on Unsaturated Soils*, Pattaya, Thailand, November.

Fredlund, M.D. (1999), "The role of unsaturated soil property functions in the practice of unsaturated soil mechanics", PhD thesis, University of Saskatchewan, Canada.

Li, Y. and Vanapalli, S.K. (2021), "A novel modeling method for the bimodal soil-water characteristic curve", *Comput. Geotech*., **138**(2021), 104318. https://doi.org/10.1016/j.compgeo.2021.104318.

Liu, Y. and Vanapalli, S.K. (2019), "Prediction of lateral swelling pressure behind retaining structure with expansive soil as backfill", *Soils Found*., **59**(1); 176-195. https://doi.org/10.1016/j.sandf.2018.10.003.

Lu, N. and Dong, Y. (2017), "Correlation between soil-shrinkage curve and water-retention characteristics", *J. Geotech. Geoenviron. Eng*., **143**(9), 04017054. https://doi.org/10.1061/(ASCE)GT.1943-5606.0001741.

Lu, N. and Khorshidi, M. (2015), "Mechanisms for soil-water retention and hysteresis at high suction range", *J. Geotech.*

Geoenviron. Eng., **141**(8), 04015032. https://doi.org/10.1061/(ASCE)GT.1943-5606.0001325.

Mitchell, J.K. and Soga, K. (2005), "Fundamentals of Soil Behavior", (Vol. 3). John Wiley and Sons, New York, USA.

Mounika, N., Raghuram, A.S.S., Basha, B.M. and Moghal, A.A.B. (2023), Effect of Hysteretic SWCC on Marappalam Rainfall-Triggered Slope Failure. (Eds., Muthukkumaran, K., Umashankar, B., Pitchumani, N.K.) Earth Retaining Structures and Stability Analysis. IGC 2021. Lecture Notes in Civil Engineering, Singapore. https://doi.org/10.1007/978-981-19-7245-4_12.

Pham, H.Q. and Fredlund, D.G. (2008), "Equations for the entire soil-water characteristic curve of a volume change soil", *Can. Geotech. J*., **45**(4), 443-453. https://doi.org/10.1139/T07-117.

Pham, H.Q., Fredlund, D.G. and Padilla, J.M. (2004), "Use of the GCTS apparatus for the measurement of soil-water characteristic curves", *Proceedings of the 57th Canadian Geotechincal Conf., 5th Joint IAH-CNC/ CGS Conf*., Quebec, Canada.

Rafi, A. (1988), "Engineering properties and mineralogical composition of expansive clays in Al-Qatif area", Ph.D. Dissertation, KFUPM, Dammam, Saudi Arabia. doi:10.3168/jds.S0022-0302(88)79586-7.

Raghuram, A.S.S., Basha, B.M. and Moghal, A.A.B. (2020), "Effect of fines content on the hysteretic behavior of water-retention characteristic curves of reconstituted soils", *J. Mater. Civil Eng*., **32**(4), 04020057. https://doi.org/10.1061/(ASCE)MT.1943-5533.000311.

Rahardjo, H., Kim, Y. and Satyanaga, A. (2019), "Role of unsaturated soil mechanics in geotechnical engineering", *Int. J. Geo-Eng*., **10**(8), 1-23. https://doi.org/10.1186/s40703-019-0104-8.

Richards, B.G. (1965), "Measurement of the free energy of soil moisture by the psychrometric technique using thermistors", In: Aitchison GD, editor. Moisture equilibria and moisture changes in soils beneath covered areas. Butterworth and Co. Ltd., Sydney, Australia.

Rong, W. and McCartney, J.S. (2021), "Undrained seismic compression of unsaturated sand", *J. Geotech. Geoenviron. Eng*., **147**(1), 04020145. https://doi.org/10.1061/(ASCE)GT.1943-5606.0002420.

Satyanaga, A., Rahardjo, H., Leong, E.C. and Wang, J.Y. (2013), "Water characteristic curve of soil with bimodal grain-size distribution", *Comput. Geotech*., **48**, 51-61. https://doi.org/10.1016/j.compgeo.2012.09.008.

Slater, D.E. (1983), "Potential expansive soils in Arabian Peninsula", *J. Geotech. Eng*., **109**(5), 744-746. https://doi.org/10.1061/(ASCE)0733-9410(1983)109:5(744).

Tavakkoli, N. and Vanapelli, S.K. (2011), "Rational approach for the design of retaining structures using the mechanics of unsaturated soils", *Proccedings of the 2011 Pan-American CGS Geotechnical Conference*, Toronto, Ontario, Canada.

Tuller, M., Or, D. and Dudley, L.M. (1999), "Adsorption and capillary condensation in porous media: Liquid retention and interfacial configurations in angular pores", *Water Resour. Res*., **35**(7), 1949-1964. https://doi.org/10.1029/1999WR900098.

Vanapalli, S.K., Fredlund, D.G., Pufahl, D.E. and Clifton, A.W. (1996), "Model for the prediction of shear strength with respect to soil suction", *Can. Geotech. J*., **33**(3), 379-392. https://doi.org/10.1139/t96-060.

Vanapalli, S.K., Sillers, W.S. and Fredlund, M.D. (1998), "The meaning and relevance of residual state to unsaturated soils", *Proceedings of the 51st Canadian Geotechnical Conference*, Edmonton. Alberta, Canada, July.

Villar, L.F.S., de Campos, T.M.P., Azevedo, R.F. and Zornberg, J.G. (2009), "Tensile strength changes under drying and its correlations with total and matric suctions", *Proceedings of the 17th International Conference of Soil Mechanics and Geotechnical Engineering*, Alexandria, Egypt, October.

Wijaya, M., Leong, E.C. and Rahardjo, H. (2015), "Effect of shrinkage on air-entry value of soils", *Soils Found*., **55**(1), 166-180. https://doi.org/10.1016/j.sandf.2014.12.013.

Zhai, Q., Rahardjo, H., Satyanaga, A. and Dai, G. (2020), "Estimation of the soil-water characteristic curve from the grain size distribution of coarse-grained soils", *Eng. Geol*., **267**, 105502. https://doi.org/10.1016/j.enggeo.2020.105502.

Zhang, L. and Chen, Q. (2005), "Predicting bimodal soil–water characteristic curves", *J. Geotech. Geoenviron. Eng*., **131**(5), 666-670. https://doi.org/10.1061/(ASCE)1090-0241(2005)131:5(666).

Zhou, B. and Lu, N. (2021), "Correlation between Atterberg limits and soil adsorptive water", *J. Geotech. Geoenviron. Eng*., **147**(2), 04020162. https://doi.org/10.1061/(ASCE)GT.1943-5606.0002463.

CC